Report of the National Research Institute for Earth Science and Disaster Prevention, No. 61 ; March, 2001

Western North Pacific Tropical Cyclones and ENSO in NIED CGCM

By

Michiaki YUMOTO*, Tomonori MATSUURA*, Ryuichi KAWAMURA, and Satoshi IIZUKA***

**National Research Institute for Earth Science and Disaster Prevention, Japan*
***Department of Earth Sciences, Faculty of Science, Toyama University, Japan*

Abstract

The influence of El Niño/Southern Oscillation (ENSO) on tropical cyclone (TC) activity in the western North Pacific (WNP) is investigated using a high-resolution atmosphere-ocean Coupled General Circulation Model (CGCM) developed by the National Reseach Institute for Earth Science and Disaster Prevention. The CGCM simulation indicates the model TC activity associating with the ENSO as follows ; (1) the frequency of model TC in the WNP during the ENSO cold phase is slightly higher than that during the ENSO warm phase, (2) the genesis location of model TC shifts eastward during the ENSO warm phase, (3) model TC tends to migrate westward during the ENSO warm phase and northward during the ENSO cold phase. These results are intimately related to variations in atmospheric circulation and SST during the ENSO. Similar influences are also confirmed in the relationship between actual TC activity and actual ENSO.

Key words : Tropical cyclone activity, El Niño/Southern Oscillation (ENSO), Coupled General Circulation Model (CGCM)

1. Introduction

Tropical cyclones (TCs) lead to serious disasters such as landslides, floods, *etc.*, and cause extensive damage to human life and the economy. For example, Typhoon 9918 BART led to a storm surge in Shiranui Town, Kumamoto Prefecture on September 24, 1999 and claimed many human lives.

Approximately 28 out of 80 TCs in the world are generated over the western North Pacific (WNP) each year (RSMC Tokyo-Typhoon Center, 1992). Moreover, we need to pay attention not only to the number of TCs but also to their courses because it is necessary to monitor their migration as a measure to prevent disasters. TCs recurving to the northeast near the Ryukyu Islands often hit Japan causing extensive damage.

It is well known that TC genesis is related to six conditions of the tropical atmosphere and ocean (Gray, 1968 ; Henderson-Sellers *et al.*, 1998 ; Lighthill *et al.*, 1994 ; Raper, 1993) ; (1) sea surface temperatures (SSTs) exceeding 26 °C to depths of about 60 m, (2) the Coriolis parameter, (3) large values of low-level relative vorticity, (4) weak vertical shear of horizontal winds, (5) conditional instability through deep atmospheric layers, and (6) large values of relative humidity in the lower and middle troposphere.

Since the SST in the WNP is 26 °C or more throughout the year, it is possible for TCs in the WNP do occasionally develop and intensify in the boreal winter and the annual number is higher than in any other basin. It is anticipated that warm SSTs enable many TCs to occur.

Warm SSTs are necessary for TC genesis, but are not a sufficient condition in isolation ; large-scale atmospheric circulation affects TC genesis. As indicated by Gray (1975), few TCs form in the vicinity of

*Tennodai 3-1, Tsukuba, Ibaraki, 305-0006, Japan
**Toyama, 930-8555, Japan

the Hawaiian Islands due to the strong shear of westerly winds. That is, the other factors are also significant, or more important, than the warm SSTs for TC genesis.

Both atmospheric and oceanic conditions exert a considerable influence on TC genesis. If the SST beneath the route of a TC is high, and the TC can receive heat energy from the surface of the ocean continuously, the TC will intensify. The trade winds and the prevailing westerly winds play important roles in the movment of a TC. The distribution of the Ogasawara high during summer through fall is also closely connected to the movement of TCs. TC activity is a local phenomenon and is also directly influenced by large-scale conditions.

El Niño/Southern Oscillation (ENSO) is the most prominent interannual phenomenon with anomalous SST variance in the eastern equatorial Pacific and the large-scale fluctuation of atmospheric pressure between the eastern and western equatorial Pacific. Many investigators have endeavored to reveal the relationship between TC activity and ENSO. It has been reported that TC activities in the western North Atlantic (WNA) and in the western South Pacific (WSP) tend to be below normal in El Niño years (Gray, 1984 ; Nicolls, 1984). This decreasing activity in the Atlantic is explained by the fact that anomalous westerly winds in the upper-troposphere over the Caribbean and the equatorial Atlantic associated with El Niño can increase both vertical shear and upper -level vorticity over the region, providing a less favorable environment for TC genesis (Gray, 1984 ; Shapiro, 1987). Two contrasting opinions on the relationship between TC activity in the WNP and ENSO exist. One is that El Niño is closely related to a decrease in the annual number of TCs in the WNP (Aoki, 1985 ; Chan, 1985 ; Li, 1988). The other is that no significant correlation exists between the annual number of TCs and ENSO (Ramage and Hori, 1981 ; Lander, 1994).

ENSO plays a major role in the interannual fluctuation of the genesis location of TCs in the WNP. Annual mean genesis location of TCs in the WNP shifts eastward during El Niño years (Chan, 1985 ; Dong, 1988 ; Lander, 1994). This variability of TC activity is explained in terms of the change in horizontal and vertical circulations in the atmosphere during an ENSO event (Chan, 1985 ; Lander, 1994).

The relationship between TC activity in the WNP and ENSO has also been investigated using a general circulation model, which is able to simulate the essential characteristics of both TC activity and the ENSO phenomena. Wu and Lau (1992), using their low -resolution general circulation model, explained the low-frequency of TC formation simulated in the WNP, WSP, and the WNA during El Niño and a seesaw effect on TC frequency between the WNP and the central North Pacific associated with ENSO, from the viewpoint of the changes in large-scale tropical circulation.

To investigate the relationship between TC activity in the WNP and ENSO therefore, we need to understand both the atmospheric and oceanic circumstances in both the warm and cold phases of ENSO, respectively. It is difficult to isolate the impact of ENSO on TC activity by using observational data alone (Wu and Lau, 1992). At the same time, the effects of changes in the general circulation of the atmosphere on ocean circulation and its consequent effects, also need to be considered. The understanding of these effects needs to be investigated using a high-resolution atmosphere-ocean Coupled General Circulation Model (CGCM).

The National Research Institute for Earth Science and Disaster Prevention (NIED) has developed a high resolution CGCM. Our CGCM is able to reproduce highly realistic TC and ENSO phenomena (Matsuura *et al.*, 1999). The purpose of this paper is to investigate the relationship between TC activity in the WNP and the ENSO phenomena using the results of CGCM simulation and detailed observations.

The next section gives an outline of our CGCM and describes the observational data used in this paper. In section 3, the model-ENSO and model TC are defined and their characteristics are shown in comparison to data from actual observations. Specifically, the performance of our CGCM is verified in Fig. 1, in which the model SST anomalies are compared to the observed SST anomalies. The trends of TC activities are examined in section 4, namely, frequency, the genesis region, and the migration in ENSO warm and cold phases, respectively. In section 5, the influences of ENSO upon TC activity are discussed. The final section is the conclusion of this paper.

2. Model description and observational data sources

The atmospheric component of our CGCM is the Global Spectral Model (GSM) 8911 developed by the Japan Meteorological Agency (JMA) for operational numerical weather prediction (JMA, 1993). The NIED has also used this Atmospheric General Circulation Model (AGCM) for studies of climate change by running it over long periods (Kawamura *et al.*, 1995). This AGCM has a 1.125°×1.125° horizontal resolution

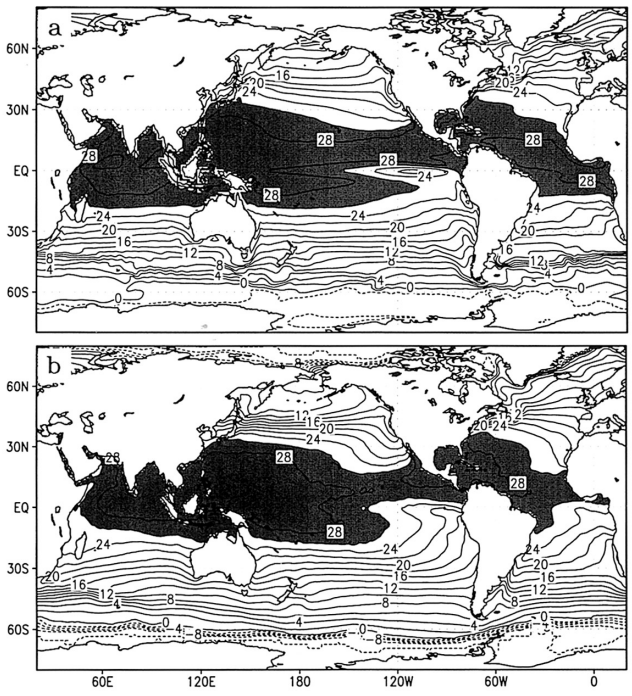

Fig. 1 Distributional patterns of SST during July to October. Oceanic areas exceeding 26 °C are shaded. The contour interval is 2 °C. (a) simulated SST of the 20-year period between Year-10 and Year-29, (b) the GISST during the period 1971-93.

(T106) and 21 levels in the vertical plane. Physics packages include the convection scheme of Kuo (1974) and Tiedtke (1985), radiation changes on a daily and seasonal basis, cloud fractions using Saito and Baba (1988), and the level 2 turbulent closure scheme by Mellor and Yamada (1974) as the planetary boundary layer process. The surface eddy fluxes of momentum, sensible heat and latent heat are computed using the bulk formulas of the stability dependence by Louis *et al.* (1982). The effect of the gravity waves induced by subgrid scale topography is parameterized according to the scheme developed by Iwasaki *et al.* (1989). The Simple Biosphere scheme (SiB) developed by Sato *et al.* (1989) is used for land surface processes.

The Oceanic General Circulation Model (OGCM) of our CGCM is the Modular Ocean Model (MOM2) of the Geophysical Fluid Dynamics Laboratory (GFDL). The horizontal resolution is 1.125° in longitude and 0.5625° in latitude. There are 37 levels in the vertical plane, with 25 of those levels in the upper 400m. Richardson number dependent diffusivity by Pacanowski and Philander (1981) is used in the vertical mixing scheme. There are no Sea Ice and River runoff processes in this OGCM.

We began the CGCM run using daily atmospheric conditions recorded on January 1, 1989, which were obtained from the integration of the AGCM from April 1, 1988 using the Meteorological Office Sea Surface Temperature (MOHSST) of the U.K. Meteorological Office (UKMO) as the boundary condition. The OGCM was spun up for 10 years from the static state using annual mean temperatures and salinity by Levitus (1982) as the initial conditions. Under these conditions, the AGCM and OGCM were coupled through daily mean SST and atmospheric fluxes. Flux correction was not used. We have integrated the data for 29 years and have analyzed the simulated results for the 20-year period from Year-10 to Year -29.

We used each set of reanalysis data from the atmosphere and ocean to evaluate the performance of our CGCM and to discuss the relationship between the actual TC activity in the WNP and ENSO. Observed SST data were obtained from the UKMO Global Ice and Sea Surface Temperature (GISST). Actual atmospheric conditions were obtained from the National Center Environmental Prediction/National Center for Atmospheric Research (NCEP/NCAR) reanalysis data (Kalnay *et al.*, 1996). Statistical data of actual TC activity in the WNP during the period 1971-93 (Table 1) was obtained from the Geophysical Review published by the JMA (1971-1993).

3. Model ENSO and model TC

3.1 Model SST anomalies and model ENSO

TCs form and develop while receiving heat energy and humidity from warm tropical oceans where the values of SST exceed 26 °C. The warm and cold phases of ENSO, namely El Niño and La Niña, are defined by the amplitude of mean SST anomalies in the NINO3 (150°W-90°W, 5°S-5°N) of the eastern tropical Pacific. It is, therefore, important to verify simulated SST data before discussing the relationship between the characteristics of model TC activity and the model-ENSO in the results of the CGCM simulation.

Fig. 1 shows the simulated and observed climatological SSTs during the typhoon season from July to October. The amplitude and spatial distribution of simulated SSTs corresponds well to those of the observed SSTs. The high resolution CGCM is able to reproduce the seasonal cycle of the warm pool exceeding 28 °C in the WNP, especially its meridianal extent during summer through fall. Another improvement is that the fine structures of intensive currents and upwelling are accurately reproduced: namely, the Kuroshio and the Gulf stream, and the upwelling east

Table 1 Monthly and annual number of actual TCs in the WNP

	Jan	Feb	Mar	Apr	May	Jun	Jul	Aug	Sep	Oct	Nov	Dec	Total	JASO
1971	1	0	1	3	4	2	8	5	6	4	2	0	36	23
1972	1	0	0	0	1	3	6	5	5	5	3	2	31	21
1973	0	0	0	0	0	0	7	5	2	4	3	0	21	18
1974	1	0	1	1	1	4	4	5	5	4	4	2	32	18
1975	1	0	0	0	0	0	2	4	5	5	3	1	21	16
1976	1	1	0	2	2	2	4	4	5	1	1	2	25	14
1977	0	0	1	0	0	1	3	3	5	5	1	2	21	16
1978	1	0	0	1	0	3	4	8	5	4	4	0	30	21
1979	1	0	1	1	2	0	4	2	6	3	2	2	24	15
1980	0	0	0	1	4	1	4	2	6	4	1	1	24	16
1981	0	0	1	2	0	3	4	8	4	2	3	2	29	18
1982	0	0	3	0	1	3	3	5	5	3	1	1	25	16
1983	0	0	0	0	0	1	3	5	2	5	5	2	23	15
1984	0	0	0	0	0	2	5	5	4	7	3	1	27	21
1985	2	0	0	0	1	3	1	8	5	4	1	2	27	18
1986	0	1	0	1	2	2	3	5	3	5	4	3	29	16
1987	1	0	0	1	0	2	4	4	6	2	2	1	23	16
1988	1	0	0	0	1	3	2	8	8	5	2	1	31	23
1989	1	0	0	1	2	2	7	5	6	4	3	1	32	22
1990	1	0	0	1	1	3	4	6	4	4	4	1	29	18
1991	0	0	2	1	1	1	4	5	6	3	6	0	29	18
1992	1	1	0	0	0	2	4	8	5	7	3	0	31	24
1993	0	0	1	0	0	1	4	7	5	5	2	3	28	21
Ave	0.6	0.1	0.5	0.7	1.0	1.9	4.1	5.3	4.9	4.1	2.7	1.3	27.3	18.4

of Peru. In our CGCM, the equatorial cold tongue tends to be too narrow and extend too far west ; this phenomena has also been observed in other CGCMs (Mechoso *et al.*, 1995). The excessive westerly extension of the model cold tongue may be caused by overly strong trade winds over the western tropical Pacific. The maximum wind stress of the trade winds over the equatorial Pacific was located at approximately 180° in the simulation ; this position is farther west than the actual position (~150°W). As the model trade winds may cause cool SSTs through equatorial upwelling in the east of the WNP and a discharge of latent heat from the ocean, the model cold tongue is too narrow and extends too far west. The other difference is that the simulated SST in the eastern North Pacific is higher than the observed SST. Warm SSTs may also be a factor in the excessively narrow cold tongue of the CGCM. There is room for improvement of SSTs and wind profiles in the development of CGCMs.

Fig. 2 shows the time series of 7-month running mean of SST anomalies and the Southern Oscillation Index (SOI) for both the model simulation and the observation. Simulated and observed monthly SST anomalies are averaged in the model NINO3 (150°W -120°W, 4°S-4°N) and in the observed NINO3 for each month, respectively. The SOI is obtained from the sea -level pressure difference between Tahiti and Darwin. In general, it is known that the SST anomalies in NINO-3 correlate with negative anomalies of the SOI in El Niño and that they correlate with positive anomalies of the SOI in La Niñas. In the observation, the correlation value (r) between the SST anomaly and SOI by 7-month running mean is strongly negative ($r=-0.85$) during the period 1971-93. In the simulation using our CGCM, the correlation value is also negative ($r=-0.62$).

The maximum and minimum values of simulated SST anomalies are +1.28 °C and −0.71 °C, respectively. The maximum value is nearly the same as the observed value of El Niño in 1987 (+1.35 °C in September) and in 1991/1992 (+1.27 °C in March 1992), and the minimum value is virtually identical to the observed value of the weak La Niña in 1985 (−0.71 °C in April). The variance of simulated SST anomalies is smaller than that of observed SST anomalies : the standard deviation of the simulated SST is 0.38 °C and that of the observed SST is 0.78 °C.

Based on the time series of the simulated SST anomalies and the simulated SOI (Fig. 2a and Fig. 2b), the definition of the model-ENSO is as follows :

1. During model-ENSOs, negative correlation should be maintained between the simulated SST anomalies and the simulated SOI,
2. During the model-ENSO warm phase, the values of the simulated SST anomalies should exceed the positive value of the standard deviation ($\sigma=+0.38$ °C), and

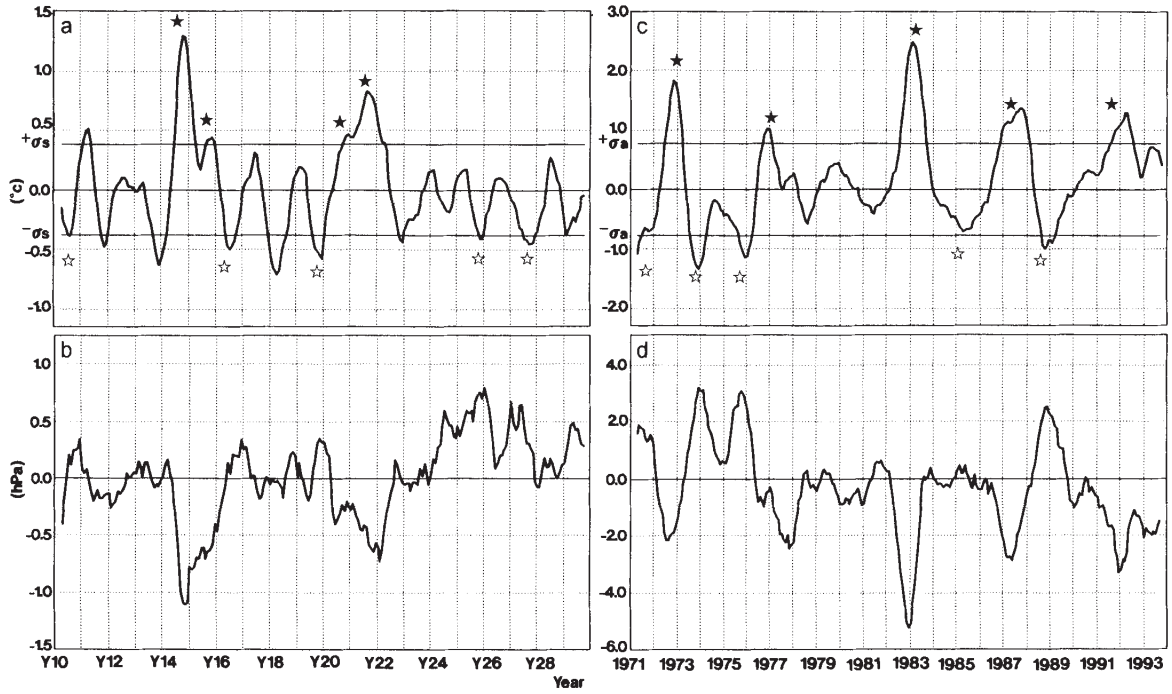

Fig. 2 Time series of (a) the simulated and (c) observed SST anomalies in NINO-3 and (b) simulated and (d) observed SOI between Darwin and Tahiti. Closed star (★) shows the ENSO warm phase and the clear star (☆) shows the ENSO cold phase. $\pm\sigma$ are standard deviation of SST anomalies.

3. During the model-ENSO cold phase, the values of the simulated SST anomalies should be below the negative value of the standard deviation ($\sigma = -0.38$ °C).

Both phenomena of the model and observed ENSO are defined by these descriptions hereafter. The model-ENSO warm phase appears in Years-11, 14, 15, and 20/21, and does not appear after Year-22. The model-ENSO cold phase appears in Years-10, 16, 19, 25, and 27.

3.2 Model TCs in the WNP

The output of the CGCM run reproduces model depressions at surface level at low latitudes. We investigated the behavior of the model depression (the physical quantities of pressure, wind speed near the center of the TC, and relative vorticity at 850 hPa) in the CGCM and defined a model TC as follows; A model TC is a Tropical Depression (TD) that has a minimum surface pressure below 1008 hPa, a maximum wind speed exceeding 17m s^{-1}, and maximum relative vorticity exceeding 1.2×10^{-4} s^{-1} at 850 hPa in the WNP between 120°E and 180°. A representative model TC has a vertical structure with (1) strong wind speeds sometimes exceeding 35m s^{-1} at 850 hPa, (2) stronger wind speeds on the right of the TC track than on the left, (3) wet air converging in the lower levels of the atmosphere, rising in the center of the TC, and diverging at 200 hPa, and (4) a warm core with a temperature anomaly exceeding 8 °C; this anomalous temperature of the model TC is identical to that of an actual TC (cf. Matsuura *et al.*, 1999). With regard to the ocean response to the model TC, strong mixing occurs from the surface to a depth of about 50m and a divergent Ekman drift is induced in the upper layers of the ocean by cyclonic wind stress, so that there is an upwelling of the seasonal thermocline beneath the center of the TC. The characteristic variation of the upper layers of the ocean beneath the model TC is similar to that beneath an actual hurricane or typhoon (Price, 1981). However, the eye of the model TC is unclear because the resolution of the atmospheric part is too coarse to reproduce the eye structure, as pointed out by Bengtsson *et al.* (1995). To reproduce a detailed structure of the eye, the horizontal resolution of the AGCM must be improved by approximately 10 -50km.

The annual mean number of model TCs in the WNP is 13.5 with a range of 6-26 (see Table 2). The maximum monthly frequency appears in August for both model and observed cases (Fig. 3). In December, the monthly number of model TCs is somewhat higher than that of actual TCs. The monthly number of model TCs for each month in the typhoon season from July to October is approximately half that of actual

Table 2 Monthly and annual number of model TCs in the WNP.

	Jan	Feb	Mar	Apr	May	Jun	Jul	Aug	Sep	Oct	Nov	Dec	Total	JASO
Y10	0	1	0	0	0	0	1	6	5	4	2	7	26	16
Y11	0	2	0	0	1	0	3	3	2	1	2	2	16	9
Y12	0	1	0	0	0	1	0	3	1	2	3	2	13	6
Y13	1	0	0	0	1	0	1	2	1	1	0	1	8	5
Y14	0	0	0	0	3	3	1	0	1	2	0	2	12	4
Y15	0	0	1	0	0	3	0	6	5	2	2	4	23	13
Y16	0	0	0	0	0	1	0	2	2	2	4	4	15	6
Y17	2	0	1	0	2	1	1	2	2	2	0	2	15	7
Y18	0	0	1	1	0	1	1	0	0	0	2	0	6	1
Y19	0	2	0	0	0	0	1	5	1	1	1	2	13	8
Y20	0	0	1	0	0	0	2	1	3	0	1	0	8	6
Y21	1	0	0	1	2	1	3	4	1	0	2	0	15	8
Y22	0	0	0	0	1	0	3	2	2	2	4	1	15	9
Y23	0	0	2	0	1	0	1	1	2	2	0	0	9	6
Y24	0	0	0	1	1	0	0	2	2	2	0	2	10	6
Y25	0	0	0	0	0	0	1	6	3	2	2	2	16	12
Y26	1	1	1	0	1	0	5	2	1	2	1	2	17	10
Y27	1	0	0	0	0	1	1	4	2	0	1	1	11	7
Y28	0	0	0	1	0	1	2	2	2	3	4	1	16	9
Y29	0	0	0	2	1	0	1	1	1	0	0	0	6	3
Ave	0.3	0.4	0.4	0.3	0.7	0.7	1.4	2.7	2.0	1.5	1.6	1.8	13.5	7.6

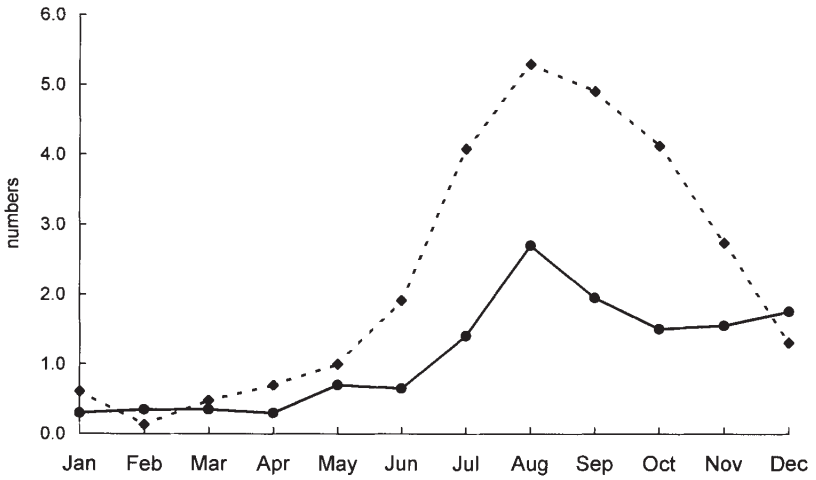

Fig. 3 Monthly average number of model TCs averaged from Year-10 to Year-29 (solid line) and that of actual TCs averaged from 1971 to 1993 (dashed line).

TCs.

In the pre-typhoon season from March to June, model TCs are driven northwestward; this route is virtually identical to that observed (Fig. 4a and Fig. 4d). However, few model TCs migrate northwards. In the typhoon season, the main route of model TCs shifts towards the north (Fig. 4b). Although more model TCs move northwards and recurve, a few model TCs migrate polewards across 30°N and pass along east-southeast Japan. In the post-typhoon season from November to February, the track of model TCs is similar to that of actual TCs (Fig. 4c and Fig. 4f): Most model TCs tend to migrate westwards, although some model TCs recurve toward the northeast.

In our simulation, few model TCs migrate polewards across the latitude line of 30°N. This tendency may also be caused by the weaker intensity of model TCs than that of actual TCs. The pressure at the center of model TCs is not able to reach the minimum pressure of actual TCs. While weaker model TCs are migrating to the mid-latitudinal regions, they rapidly decrease in intensity, because the TCs do not receive heat energy from the ocean due to relatively cool SSTs, for example. The reason for the weaker model TCs may be due to the coarse horizontal resolution of the atmospheric part in the CGCM.

The tendency for both model and actual TCs to

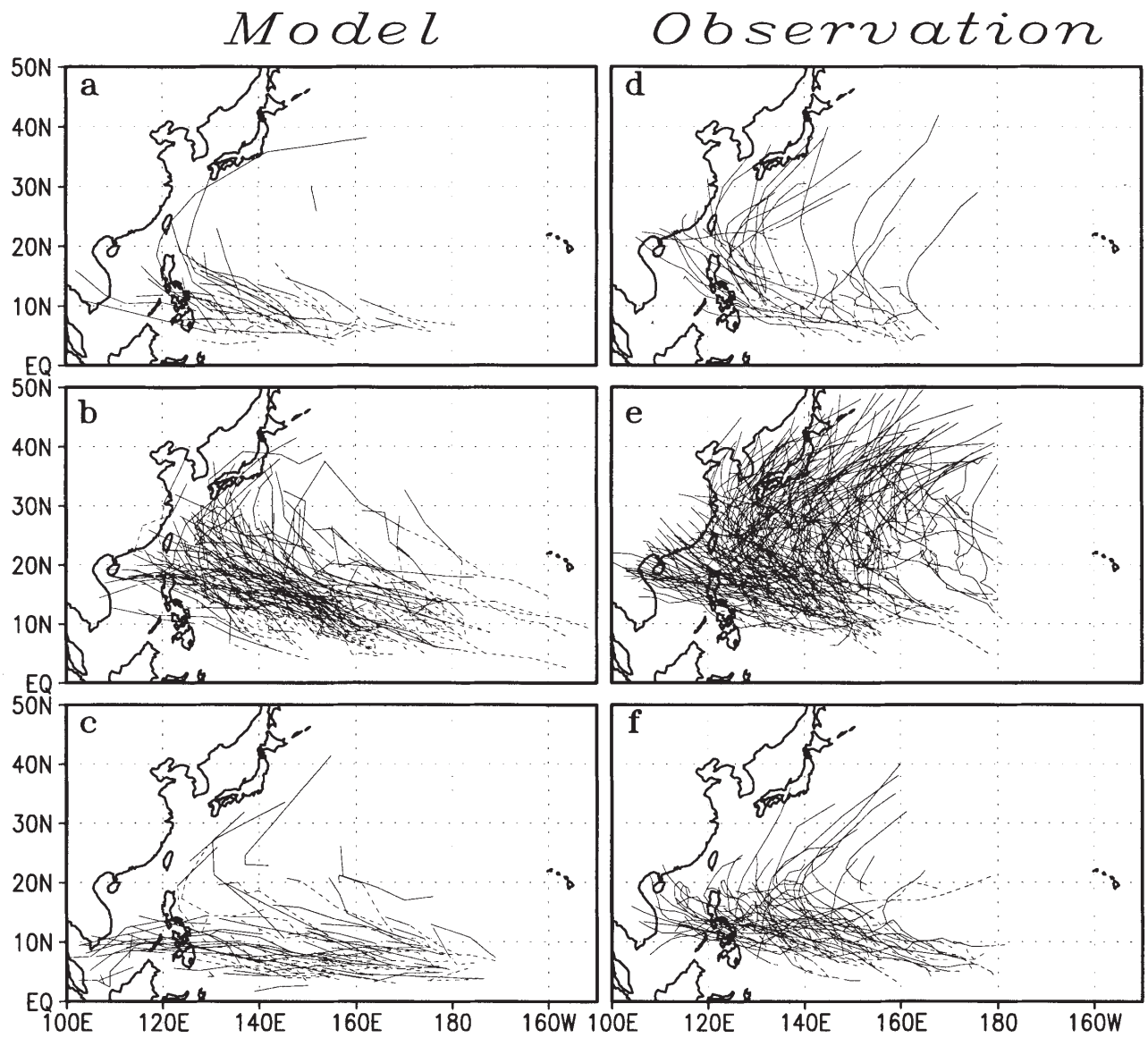

Fig. 4 Tracks of model TCs in (a) the pre-typhoon season from March to June, (b) the typhoon season form July to October, and (c) the post-typhoon season from November to February during the period Year-10 to Year-29, and those of actual TCs in (d) the pre-typhoon season, (e) the typhoon season, and (f) the post-typhoon season from 1981 to 1993. Solid line : tracks of TCs, Dashed line : tracks of TDs that develop into TCs thereafter.

migrate westward is weakest in the typhoon season. This is due to the wind system over the WNP and the TC intensity ; in the typhoon season trade winds are weaker than during the other two seasons and the winds blow in a westerly direction in the lower levels of the atmosphere over the Philippines. In the simulation, however, these westerly monsoon winds do not extend over the Philippines. Since the TC intensity is strong in the typhoon season, the non-linear effect of the TC is more intense. Therefore, the northward migrational component caused by the non-linear effect is more important (Chan and Williams, 1987).

4. TC activity in ENSO

The annual average number of model TCs in the model-ENSO warm phase years is 14.5 and that in the model-ENSO cold phase years is 16.2. The average numbers of model TCs in the typhoon season are 7.8 for the model-ENSO warm phase years and 9.8 for the model-ENSO cold phase years, respectivly (Table 3). During the 23-year period 1971-93, the annual average number of actual TCs in El Niño years was 26.6 and that in La Niña years was 27.2. In the typhoon season, the average numbers of actual TCs were 17.0 for El Niño years and 19.6 for La Niña years, respectivly. Both model and actual TC frequencies for ENSO

Table 3 Monthly and annual mean numbers of model and actual TCs during ENSO.

	Jan	Feb	Mar	Apr	May	Jun	Jul	Aug	Sep	Oct	Nov	Dec	Total	JASO
model-ENSO Warm Phase (Years-14,15,20,21)	0.3	0.0	0.5	0.3	1.3	1.8	1.5	2.8	2.5	1.0	1.3	1.5	14.5	7.8
model-ENSO Cold Phase (Years-10,16,19,25,27)	0.2	0.6	0.0	0.0	0.0	0.4	0.8	4.6	2.6	1.8	2.0	3.2	16.2	9.8
El Niño (1972,1976,1982,1987,1991)	0.6	0.2	1.0	0.8	1.0	2.2	4.2	4.6	5.4	2.8	2.6	1.2	26.6	17.0
La Niña (1971,1973,1975,1985,1988)	1.0	0.0	0.2	0.6	1.2	1.6	4.0	6.0	5.2	4.4	2.2	0.8	27.2	19.6

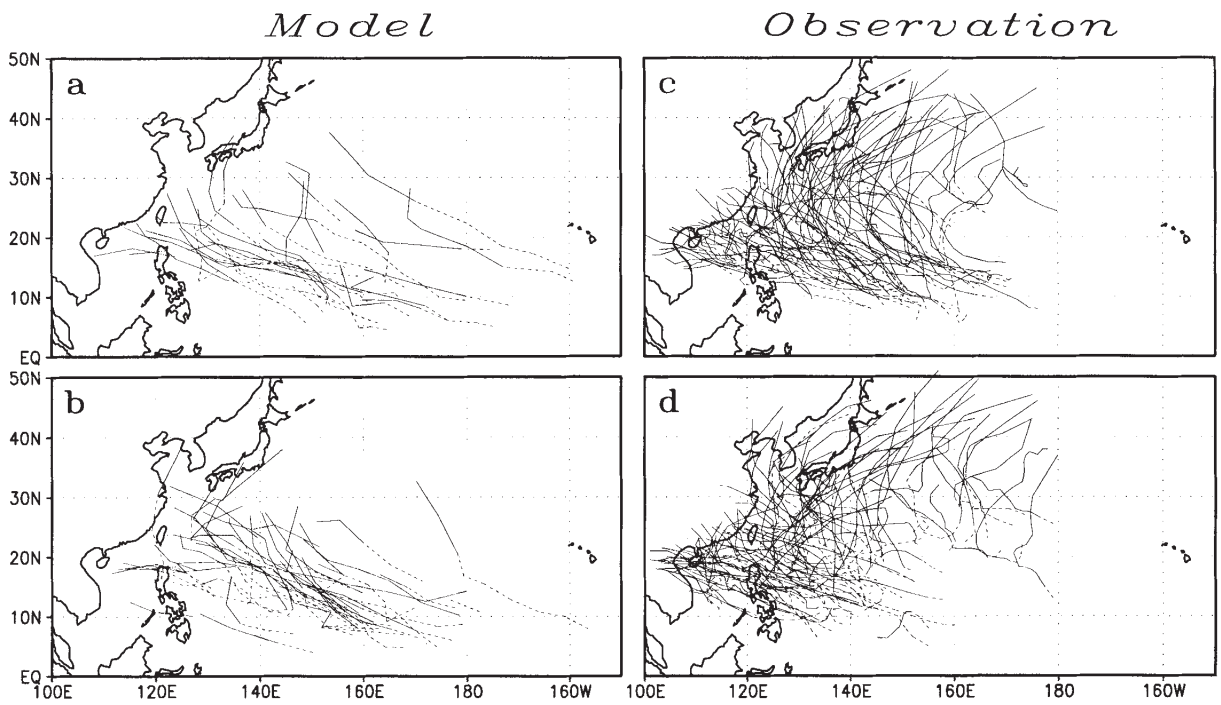

Fig. 5 Tracks of model TCs during the typhoon season in (a) the model-ENSO warm phase and (b) the model-ENSO cold phase, and those of actual TCs in (c) El Niño years (1972, 1976, 1982, 1987) and (d) La Niña years (1971, 1973, 1975, 1985, 1988). Solid line : tracks of TCs, Dashed line : tracks of TDs.

warm phase years are slightly lower than those for ENSO cold phase years.

Fig. 5 shows the trajectory of model and actual TCs for the ENSO warm and cold phases. The majority of TDs that develop into TCs thereafter (dashed lines) and TCs (solid lines) move somewhere between the west and the north. Some model TDs and one model TC occured east of the date line during the model -ENSO warm phases. The majority of the model TDs and model TCs, excluding two TDs, occured over the WNP during the ENSO cold phase. The mean longitudes of the genesis locations of model TCs are 149.8° E for the model-ENSO warm phases and 146.5°E for the model-ENSO cold phases, respectively. The genesis mean location of model TCs shifts eastwards during the model-ENSO warm phases. This expanding of the TC genesis area is also confirmed by observations during El Niño years.

In the comparison of TC tracks, model TCs prefer to move polewards during the model-ENSO cold phases rather than during the model-ENSO warm phases. During the model-ENSO warm phases the majority of the model TCs which move polewards over the WNP on the eastern side of 140°E form and develop mainly in September, and the model TCs in July, August and October move towards the west and west-northwest throughout their life spans. During the model-ENSO cold phases, the model TCs usually move towards the west-northwest or the northwest, and some model TCs move northwestward or polewards from August to October. The model TCs tend to move westwards during the model-ENSO warm phases and polewards during the model-ENSO cold phases.

In El Niño years, many actual TCs move polewards and frequently hit Japan (Fig. 5c). In La Niña years, actual TCs turn eastwards and some hit Japan (Fig. 5d). Additionally, there is a trend for the actual TCs generated over the eastern region of the WNP during the La Niña years to move towards the north.

5. Discussion

In section 4, we have described TC activities (the frequency, the genesis location, and the track) using the results of CGCM simulation and observation during both ENSO warm and cold phases. TC genesis is closely associated with global environmental conditions. To discuss the relationship between the characteristics of TC activity and ENSO, therefore, we need to understand the variations of the oceanic and atmospheric fields in the WNP during the ENSO events.

In general, the oceanic area to the east of the Philippines is an area with high TC activity. Model SSTs east of the Philippines during the model-ENSO warm phase are slightly lower than those during the model-ENSO cold phase (Fig. 6a). Although simulated SSTs between 15°N and 30°N in the WNP during model-ENSO warm phases are higher than during model-ENSO cold phases, in the atmosphere, anticyclonic circulation prevails at 850 hPa (Fig. 7b) and the geopotential height of 1000 hPa is high (Fig. 8a). That is, this shows that the anticyclonic circulation and anomalous anticyclone areas are not capable of converging wet air in low-levels of the atmosphere over oceanic areas. These oceanic and atmospheric conditions in the simulation inhibit model TC forma-

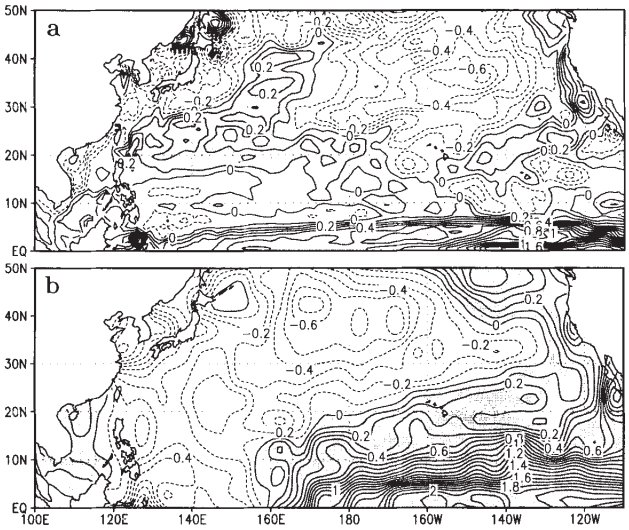

Fig. 6 Composite differences in SST between the ENSO warm and cold phases during the typhoon season. (a) CGCM simulation and (b) GISST. Shading depicts positive values. A positive value is a higher SST during the ENSO warm phase. The contour interval is 0.1 °C.

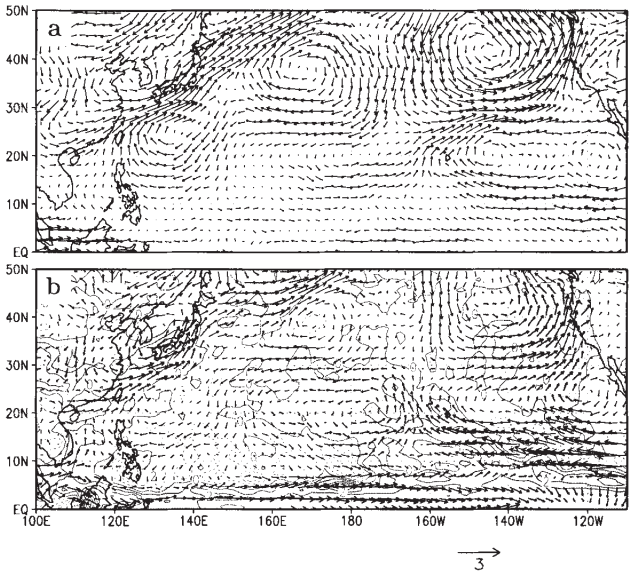

Fig. 7 Composite differences in simulated wind vectors at (a) 500 hPa and (b) 850 hPa, and precipitation between the model-ENSO warm and cold phases during the typhoon season. The contour interval for the difference of precipitation is 1 mm day^{-1}; shading depicts positive values.

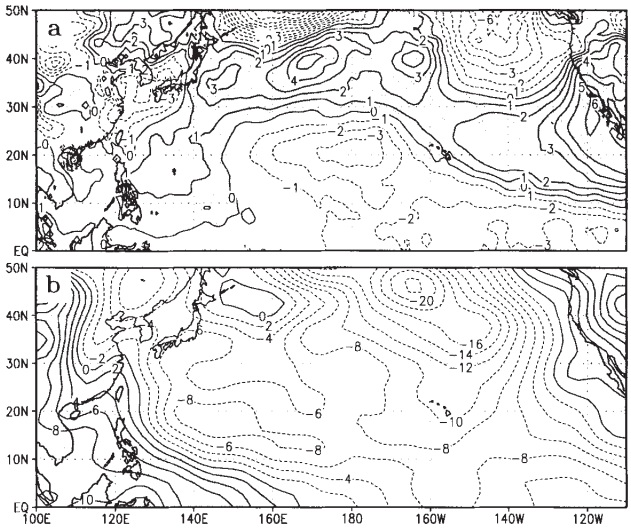

Fig. 8 Composite differences in geopotential height of 1000 hPa between the ENSO warm and cold phases duirng the typhoon season. (a) CGCM simulation and (b) the NCEP/NCAR reanalysis data. Shading depicts positive values. Positive values are higher during the ENSO warm phase. The contour intervals are 1 m for the simulation and 2 m for the NCEP/NCAR reanalysis.

tion and development over the western regions of the WNP during the model-ENSO warm phase. In the observation, the differences of SSTs were negative in the western tropical Pacific (120°E-160°E, 0°-20°N in Fig. 6b). In both CGCM simulation and observation, the frequency of TCs in the western WNP is low during the ENSO warm phase.

In the ENSO warm phase the genesis mean location of TC shifts towards the east, and the eastern end of the genesis area extends further eastward. This eastward extension of the genesis area corresponds to the easterly extension of anomalous positeve SST in the equatorial Pacific, which is associated with anomalous westerly winds during the ENSO warm phase.

The increase of anomalous positive SST causes active convection over the oceanic areas. Strong anomalous equatorial westerly winds of 850 hPa extend eastwards to 140°W in the simulation (Fig. 7b) and 120°W in the observation (Fig. 9b) during the ENSO warm phase. The eastern equatorial Pacific is associated with an anomalous divergence of 200 hPa (not shown). Simultaneously, the geopotential height of 1000 hPa indicates an anomalous low over the eastern equatorial Pacific (Fig. 8). Over the eastern equatorial Pacific, wet air converges at low levels in the atmosphere, rises, and diverges in the upper levels of the atmosphere during the ENSO warm phase. The distribution of anomalous precipitation correlates positively to that of the anomalous cyclones (Fig. 7b) and that of anomalous positive SST in the simulation. The difference of precipitation is positive in the eastern part of the WNP in the equatorial direction at 30°N and is negative in the western part. This figure shows that the Walker circulation shifts eastwards, and simultaneously supports the tendency for TCs to form over the eastern part of the WNP. During El Niño, the area of anomalous positive outgoing longwave radiation (OLR) over 10 W m^{-2} also covers southeastern Taiwan and the sea area between 140°E to 160°E and 18°N to 20°N (Fig. 9b). This suggests that the convection is less active during El Niño compared to that during La Niña. On the other hand, the area between 150°E to 170°W along 10°N indicates anomalous negative OLR. The convection over the eastern WNP is more active during El Niño and TCs occur more easily under these conditions.

Gray (1979) pointed out that TC formation needs a weak vertical shear. Fig. 10 shows that distribuions of the zonal wind vertical shear between 850 hPa and 200 hPa during the typhoon season. During the model -ENSO warm phase, vertical shear of between 160°E and 180° is extremely intense and the weak vertical

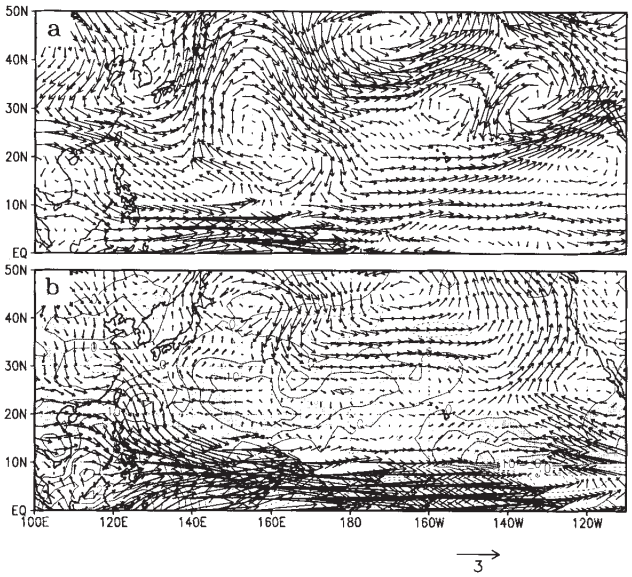

Fig. 9 Composite differences in observed wind vectors at (a) 500 hPa and (b) 850 hPa, and OLR between the the El Niño years and the La Niña years during the typhoon season. The data used is the NCEP/NCAR reanalysis data. The contour interval for OLR anomalies is 5 W m^{-2} ; shading depicts negative values.

shear region is located towards the equator at 10°N of the central equatorial Pacific. During the model -ENSO cold phase, the weak vertical shear region shifts westward, although a part of the weak shear region distributed towards the east at 180°, anomalous negative SST and an anomalous anticyclone are not necessary for TC formation there. In an actual case the difference of distribution of the weak vertical shear is shown more clearly than in the results of the simulation ; the weak vertical shear region towards the equator at 10°N extends towards the extreme east during El Niño (see Fig. 10). There are few actual TCs in the southeast region of the WNP between 160°E and 180°, towards the equator at 20°N during La Niña years (Fig. 5d). This lower frequency corresponds to strong vertical shear in oceanic areas. These oceanic and atmospheric conditions, which represent anomalous positive SST and an anomalous cyclone in the eastern equatorial Pacific and weak vertical shear extending eastwards, cause the genesis location of TCs to move eastwards during ENSO warm phases.

Model TCs tend to move westward during the model-ENSO warm phase and polewards during the model-ENSO cold phase. At 500 hPa over the location of 135°E and 25°N near Japan, anomalous anticyclonic circulation appears in the model-ENSO

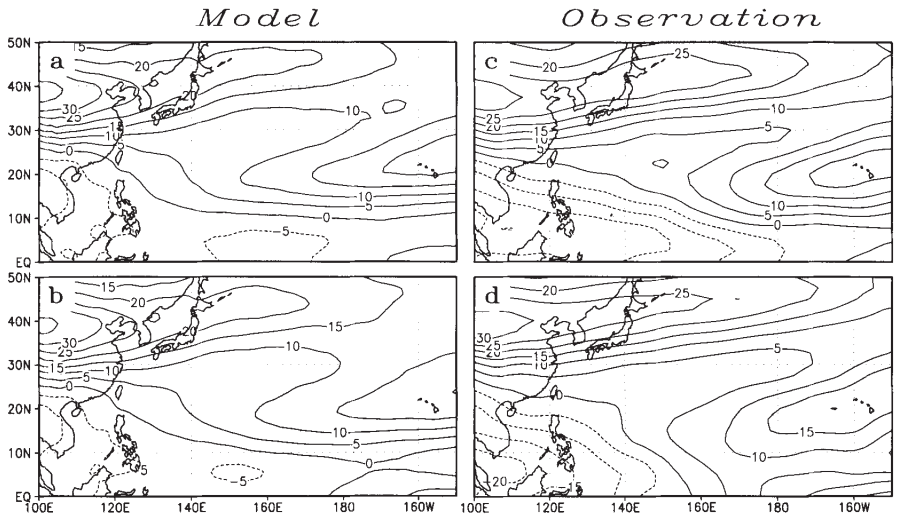

Fig. 10 Distribuions of the zonal wind vertical shear between 850 hPa and 200 hPa during the typhoon season in (a) the model-ENSO warm phase, (b) the model-ENSO cold phase, (c) El Niño years, and (d) La Niña years.

warm phase (Fig. 7a). This anomalous anticyclonic circulation prevents model TCs from moving polewards and induces model TCs to move westward during the model-ENSO warm phase. Since this anomalous circulation changes anticyclonic circulation into cyclonic circulation during the model-ENSO cold phase, model TCs are able to move polewards easily. In the observation, anomalous anticyclonic circulation exists over the location at approximately 155°E and 25°N southeast of Japan (Fig. 9a). During El Niño, an actual TC is able to move polewards passing off Japan, because it is driven by southerly winds from anomalous anticyclonic circulation. On the other hand, during La Niña years the anomalous circulation is cyclonic, and anomalous southeasterly winds develop over the region at 160°E-180° and 20°N-30°N. The anomalous southeasterly wind induces poleward movement over the region eastwards at 160°E. The anomalous circulation, which influences the movement of TC, exists over the region from 20°N to 50°N off Japan. The difference in the trajectory of actual TCs between El Niño and La Niña does not appear as clearly as in that of model TCs, since the observed anomalous circulation shifts further east than that in the simulation. This difference in the position of the anomalous circulation is due to the difference of the response of the atmosphere in ENSO between simulation and observation.

6. Conclusion

We have investigated the relationship between TC activity in the WNP and ENSO using the 20-year integrations by a high-resolution CGCM, and observational data during the period 1971-93. The CGCM could simulate the phenomena of TC activity and ENSO simultaneously. In this CGCM run, the following results on the relationship between TC activity and ENSO were obtained. The average number of model TCs both annually and in the typhoon season from July to October during the model-ENSO warm phase was slightly less than that during the model -ENSO cold phase. The genesis location of model TCs extends towards the east during the model -ENSO warm phase as does actual TC genesis. The tendencies for decreases in the number and for the genesis location of model TCs to extend towards the east are also confirmed in the observational data during El Niño years. The behavior of model TC activity is characterized by a tendency for westward migration in the model-ENSO warm phase and poleward migration in the model-ENSO cold phase. The anomalous anticyclonic circulation at 500 hPa height exists in the WNP near Japan both in simulation. The circulation influenes the migration of model TCs. However, although the anomalous anticyclonic circulation at 500 hPa height also exists southeast of Japan in the observation, the difference in the trajectory of actual TCs between El Niño and La Niña does not appear as clearly as in that of the model TCs.

Acknowledgments

We would like to express our gratitude to the Japan Meteorological Agency for providing us with the GSM 8911 code and the GFDL for providing us with the code for the MOM 2. Numerical calculations were carried out on the CRAY T932 supercomputer at the

National Research Institute for Earth Science and Disaster Prevention.

References

1) Aoki, T. (1985) : A climatological study of typhoon formation and typhoon frequency in Japan. Pap. in Meteor. and Geophys., **36**, 61-118.
2) Bengtsson, L., M. Botzet and M. Esch (1995) : Hurricane-type vortices in a general circulation model. Tellus, **47A**, 175-196.
3) Chan, J. C. L. (1985) : Tropical cyclone activity in the northwest Pacific in relation to the El Niño/Southern Oscillation phenomenon. Mon. Wea. Rev., **113**, 599-606.
4) Chan, J. C. L. and R. T. Williams (1987) : Analytical and numerical studies of the beta-effect in tropical cyclone motion. Part I : Zero mean flow. J. Atmos. Sci., **49**, 1257-1265.
5) Dong, K. (1988) : El Niño and tropical cyclone frequency in the Australian region and the northwest Pacific. Aust. Meteor. Mag., **36**, 219-255.
6) Gray, W. M. (11968) : Global view of the origin of tropical disturbances and storms. Mon. Wea. Rev., **96**, 669-700.
7) Gray, W. M. (1975) : Tropical cyclone genesis. Atmospheric Science Paper. No. **24**, Department of Atmospheric Science, Colorado State University.
8) Gray, W. M. (1979) : Hurricanes : Their formation, structure and likely role in tropical circulation. *In* : Shaw, D. B. (*ed.*), Meteorology over the Tropical Oceans. Roy. Meteor. Soc., 155-218.
9) Gray, W. M. (1984) : Atlantic seasonal hurricane frequency Part 1 : El Niño and 30 mb Quasi-Biennial Oscillation influences. Mon. Wea. Rev., **112**, 1649-1668.
10) Henderson-Sellers, A., H. Zhang, G. Berz, K. Emanuel, G. Gray, C. Landsea, G. Holland, J. Lighthill, S.-L. Shieh, P. Webster, and K. McGuffie (1998) : Tropical cyclones and global climate change : A post-IPCC assessment. Bull. Amer. Meteor. Soc., **79**, 19-38.
11) Iwasaki, T., S. Yamada and K. Tada (1989) : A parameterization scheme of orographic gravity wave drag with the different vertical partitioning, part I : Impact on medium range forecasts. J. Meteor. Soc. Japan, **67**, 11-27.
12) Japan Meteorological Agency (1971-1993) : Geophysical Review. Nos. 857-1132 (in Japanese).
13) Kalnay, E., M. Kanamitsu, R. Kistler, W. Collins, D. Deaven, L. Gandin, M. Iredell, S. Saha, G. White, J. Woollen, Y. Zhu, M. Chelliah, W. Ebisuzaki, W. Higgins, J. Janowiak, K. C. Mo, C. Ropelewski, J. Wang, A. Leetmaa, R. Reynolds, R. Jenne, and D. Joseph (1996) : The NCEP/NCAR 40-year reanalysis project. Bull. Amer. Meteor. Soc., **77**, 438-471.
14) Kawamura, R., M. Sugi and N. Sato (1995) : Interdecadal and interannual variability in the northern extratropical circulation simulated with the JMA Global Model. Part 1 : wintertime leading mode. J. Clim. 8, 3006-3019.
15) Kuo, H. L. (1974): Further studies of the influence of cumulus convection on large scale flow. J. Atmos. Sci., **31**, 1232-1240.
16) Lander, M. A. (1994) : An exploratory analysis of the relationship between tropical storm formation in the western North Pacific and ENSO. Mon. Wea. Rev., **122**, 636-651.
17) Levitus, S. (1982) : Climatological atlas of the world, NOAA Prof. Paper 13 US Govt. Print off, Washington D.C.
18) Li, C. (1988) : Actions of typhoons over the western Pacific (including the South China Sea) and El Nino. Adv. Atmos. Sci., **5**, 107-115.
19) Lighthill, J., G. Holland, W. Gray, C. Landsea, G. Craig, J. Evans, Y. Kurihara, and C. Guard (1994) : Global climate change and tropical cyclones. Bull. Amer. Meteor. Soc., **75**, 2147-2157.
20) Louis, J., M. Tiedtke and J. Geleyn (1982) : A short history of PBL parameterization at ECMWF. *In* : ECMWF Workshop on Planetary Boundary Layer Parameterization, Reading, UK, 59-80.
21) Matsuura, T., M. Yumoto, S. Iizuka and R. Kawamura (1999) : Typhoon and ENSO simulation using a high-resolution CGCM. Geophys. Res. Lett., **26**, 1755-1758.
22) Mechoso, C. R., A. W. Robertson, N. Barth, M. K. Davey, P. Delecluse, P. R. Gent, S. Ineson, B. Kirtman, M. Latif, H. L. Treut, T. Nagai, J. D. Neelin, S. G. H. Philander, J. Polcher, P. S. Schope, T. Stockdale, M. J. Cuarez, L. Terray, O. Thual, and J. J. Tribbia (1995) : The seasonal cycle over the tropical Pacific in Coupled Ocean-Atmosphere General Circulation Models. Mon. Wea. Rev., **123**, 2825-2838.
23) Mellor, G. L. and T. Yamada (1974) : A hierarchy of turbulence closure models for planetary boundary layers. J. Atmos. Sci., **31**, 1791-1806.
24) Nicholls, N. (1984) : The Southern Oscillation, sea-surface-temperature, and interannual fluctuations in Australian tropical cyclone activity. J. Clim., **4**, 661-670.
25) Pacanowski, R. C., and S. G. H. Philander (1981) : Parameterization of vertical mixing in numerical models of tropical oceans. J. Phys. Oceanogr., **111**, 1443-1451.
26) Price, J. F. (1981) : Upper ocean response to a hurricane. J. Phys. Oceanogr., **11**, 153-175.
27) Ramage, C. S. and A. M. Hori (1981) : Meteorological

aspects of El Niño. Mon. Wea. Rev., **109**, 1827-1835.

28) Raper, S. C. B. (1993): Observational data on the relationships between climatic change and the frequency and magnitude of severe tropical cyclones *In*: Warrick, R. A., E. M. Barrow and T. M. L. Wigley (*eds.*), Climate and Sea level change. Observations, Projections and Implications. Cambridge University Press, 192-212.

29) RSMC Tokyo-Typhoon Center (1992): Tropical cyclone tracks in the western North Pacific 1951-1990. Japan Meteologocal Agency.

30) Saito, K. and A. Baba (1988): A statistical relationship between relative humidity and the GMS observed cloud amount. J. Meteor. Soc. Japan, **66**, 187-192.

31) Sato, N., P. J. Sellers, D. A. Randall, E. K. Scheneider, J. Shukla, J. L. Kinter III, Y. T. Hou, and E. Albertazzi (1989): Effects of implementing the simple biosphere model in a general circulation model. J. Atmos. Sci., **46**, 2757-2782.

32) Shapiro, L. J. (1987): Month-to-month variability of the Atlantic tropical circulation and its relationship to tropical storm formation. Mon. Wea. Rev., **115**, 2598-2614.

33) Tiedtke, M. (1985): The sensitivity of the time-mean large-scale flow to cumulus convection in the ECMWF model. *In*: ECMWF Workshop on convection in large-scale numerical models, Reading, England, 297-316.

34) Wu, G. and N. C. Lau (1992): A GCM simulation of the relationship between tropical-storm formation and ENSO. Mon. Wea. Rev., **120**, 958-977.

(Accepted: November 17, 2000)

Report of the National Research Institute for Earth Science and Disaster Prevention, No. 61 ; March, 2001

防災科学技術研究所の大気海洋結合モデルにおける北西太平洋の熱帯低気圧とENSO

湯本道明*・松浦知徳*・川村隆一**・飯塚　聡*

*防災科学技術研究所　気圏・水圏地球科学技術研究部
**富山大学　理学部

要　旨

防災科学技術研究所で開発された高解像度大気海洋結合モデルを用いて，エルニーニョ南方振動(ENSO)が台風の発生頻度や発生位置および移動経路に対してどのような影響を与えているかを検討した．結合モデルはENSOおよび台風のどちらの現象と実際の現象をよく再現していた．モデルで再現された台風の発生頻度は，ENSOの暖かいフェーズの時よりも冷たいフェーズの時の方がやや多い．モデル台風の発生域は，ENSOの暖かいフェーズの時の方が冷たいフェーズの時よりも東に広がる．モデルの台風の移動経路は，ENSOの暖かいフェーズで西進の傾向が，冷たいフェーズで北上傾向が顕著になる．ENSOによって発生域が東に広がることと移動経路に相違があることは，ENSOによって低緯度域の大気の循環と海水面温度の分布が変動することに起因する．

キーワード：熱帯低気圧活動，エルニーニョ南方振動（ENSO），大気海洋結合モデル